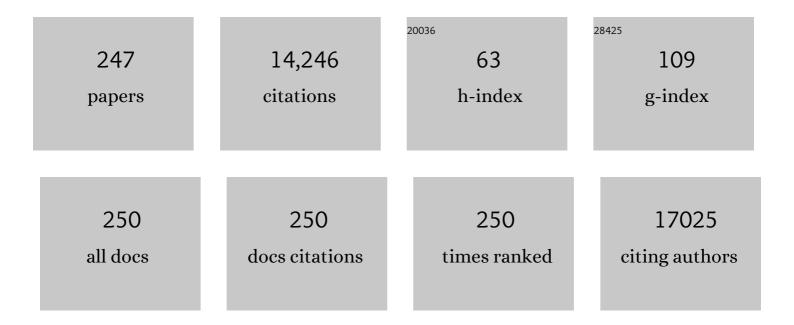
List of Publications by Year in descending order

Source: https://exaly.com/author-pdf/1883704/publications.pdf Version: 2024-02-01



#	Article	IF	CITATIONS
1	The Usefulness of Ultrasound Surveillance for Axillary Recurrence in Women With Personal History of Breast Cancer, 2022, 25, 25.	0.8	2
2	lpsilateral Lymphadenopathy After COVID-19 Vaccination in Patients With Newly Diagnosed Breast Cancer. Journal of Breast Cancer, 2022, 25, 131.	0.8	6
3	Added value of ultrafast sequence in abbreviated breast MRI surveillance in women with a personal history of breast cancer: A multireader study. European Journal of Radiology, 2022, 151, 110322.	1.2	6
4	US Evaluation of Axillary Lymphadenopathy Following COVID-19 Vaccination: A Prospective Longitudinal Study. Radiology, 2022, 305, 46-53.	3.6	18
5	Microcalcifications and Peritumoral Edema Predict Survival Outcome in Luminal Breast Cancer Treated with Neoadjuvant Chemotherapy. Radiology, 2022, 304, 310-319.	3.6	15
6	Glandular Tissue Component on Breast Ultrasound in Dense Breasts: A New Imaging Biomarker for Breast Cancer Risk. Korean Journal of Radiology, 2022, 23, 574.	1.5	6
7	Abbreviated Screening MRI for Women with a History of Breast Cancer: Comparison with Full-Protocol Breast MRI. Radiology, 2022, 305, 36-45.	3.6	16
8	Acquisition and Interpretation Guidelines of Breast Diffusion-Weighted MRI (DW-MRI): Breast Imaging Study Group of Korean Society of Magnetic Resonance in Medicine Recommendations. Investigative Magnetic Resonance Imaging, 2022, 26, 83.	0.2	2
9	Diffusion-weighted Breast MRI in Prediction of Upstaging in Women with Biopsy-proven Ductal Carcinoma in Situ. Radiology, 2022, 305, 307-316.	3.6	10
10	Simultaneous Multislice Readoutâ€Segmented Echo Planar Imaging for <scp>Diffusionâ€Weighted MRI</scp> in Patients With Invasive Breast Cancers. Journal of Magnetic Resonance Imaging, 2021, 53, 1108-1115.	1.9	25
11	Theranostics for Breast Cancer Stem Cells. Advances in Experimental Medicine and Biology, 2021, 1187, 267-281.	0.8	2
12	Diffusion-Weighted Magnetic Resonance Imaging of the Breast: Standardization of Image Acquisition and Interpretation. Korean Journal of Radiology, 2021, 22, 9.	1.5	33
13	Prediction of axillary nodal burden in patients with invasive lobular carcinoma using MRI. Breast Cancer Research and Treatment, 2021, 186, 463-473.	1.1	8
14	Diffusion-Weighted Magnetic Resonance Imaging for Breast Cancer Screening in High-Risk Women: Design and Imaging Protocol of a Prospective Multicenter Study in Korea. Journal of Breast Cancer, 2021, 24, 218.	0.8	8
15	Comparison of Abbreviated MRI and Full Diagnostic MRI in Distinguishing between Benign and Malignant Lesions Detected by Breast MRI: A Multireader Study. Korean Journal of Radiology, 2021, 22, 297.	1.5	11
16	Automated breast US as the primary screening test for breast cancer among East Asian women aged 40–49 years: a multicenter prospective study. European Radiology, 2021, 31, 7771-7782.	2.3	5
17	Cancerâ€associated fibroblasts induce an aggressive phenotypic shift in nonâ€malignant breast epithelial cells via interleukinâ€8 and S100A8. Journal of Cellular Physiology, 2021, 236, 7014-7032.	2.0	15
18	Noncontrastâ€Enhanced MR â€Based Conductivity Imaging for Breast Cancer Detection and Lesion Differentiation. Journal of Magnetic Resonance Imaging, 2021, 54, 631-645.	1.9	8

#	Article	IF	CITATIONS
19	Factors Affecting Pathologic Complete Response Following Neoadjuvant Chemotherapy in Breast Cancer: Development and Validation of a Predictive Nomogram. Radiology, 2021, 299, 290-300.	3.6	44
20	Interval Cancers after Negative Supplemental Screening Breast MRI Results in Women with a Personal History of Breast Cancer. Radiology, 2021, 300, 314-323.	3.6	12
21	Glandular Tissue Component and Breast Cancer Risk in Mammographically Dense Breasts at Screening Breast US. Radiology, 2021, 301, 57-65.	3.6	10
22	Application of immunotherapy based on dendritic cells stimulated by tumor cell-derived exosomes in a syngeneic breast tumor mouse model. Biochemistry and Biophysics Reports, 2021, 28, 101136.	0.7	2
23	Diffusion-Weighted Imaging as a Stand-Alone Breast Imaging Modality. Journal of the Korean Society of Radiology, 2021, 82, 29.	0.1	Ο
24	Detection of Contralateral Breast Cancer Using Diffusion-Weighted Magnetic Resonance Imaging in Women with Newly Diagnosed Breast Cancer: Comparison with Combined Mammography and Whole-Breast Ultrasound. Korean Journal of Radiology, 2021, 22, 867.	1.5	6
25	Histological Findings of Mammary Gland Development and Risk of Breast Cancer in <i>BRCA1</i> Mutant Mouse Models. Journal of Breast Cancer, 2021, 24, 455.	0.8	2
26	Imaging Protocol and Criteria for Evaluation of Axillary Lymph Nodes in the NAUTILUS Trial. Journal of Breast Cancer, 2021, 24, 554.	0.8	9
27	Noninvasive Photoacoustic Imaging of Dendritic Cell Stimulated with Tumor Cell-Derived Exosome. Molecular Imaging and Biology, 2020, 22, 612-622.	1.3	10
28	Combined the SMAC mimetic and BCL2 inhibitor sensitizes neoadjuvant chemotherapy by targeting necrosome complexes in tyrosine aminoacyl-tRNA synthase-positive breast cancer. Breast Cancer Research, 2020, 22, 130.	2.2	7
29	Prediction of pathologic complete response using image-guided biopsy after neoadjuvant chemotherapy in breast cancer patients selected based on MRI findings: a prospective feasibility trial. Breast Cancer Research and Treatment, 2020, 182, 97-105.	1.1	36
30	Diffusion-weighted MRI at 3.0 T for detection of occult disease in the contralateral breast in women with newly diagnosed breast cancer. Breast Cancer Research and Treatment, 2020, 182, 283-297.	1.1	12
31	Automated Breast Ultrasound Screening for Dense Breasts. Korean Journal of Radiology, 2020, 21, 15.	1.5	44
32	Time-to-enhancement at ultrafast breast DCE-MRI: potential imaging biomarker of tumour aggressiveness. European Radiology, 2020, 30, 4058-4068.	2.3	30
33	Supplemental Breast US Screening in Women with a Personal History of Breast Cancer: A Matched Cohort Study. Radiology, 2020, 295, 54-63.	3.6	13
34	Automated Breast Ultrasound System for Breast Cancer Evaluation: Diagnostic Performance of the Two-View Scan Technique in Women with Small Breasts. Korean Journal of Radiology, 2020, 21, 25.	1.5	14
35	Computerâ€eided diagnosis of breast ultrasound images using ensemble learning from convolutional neural networks. Computer Methods and Programs in Biomedicine, 2020, 190, 105361.	2.6	143
36	Axillary Nodal Evaluation in Breast Cancer: State of the Art. Radiology, 2020, 295, 500-515.	3.6	151

#	Article	IF	CITATIONS
37	Ultrafast Dynamic Contrast-Enhanced Breast MRI: Lesion Conspicuity and Size Assessment according to Background Parenchymal Enhancement. Korean Journal of Radiology, 2020, 21, 561.	1.5	19
38	Utility and Diagnostic Performance of Automated Breast Ultrasound System in Evaluating Pure Non-Mass Enhancement on Breast Magnetic Resonance Imaging. Korean Journal of Radiology, 2020, 21, 1210.	1.5	2
39	Detection of noncalcified breast cancer in patients with extremely dense breasts using digital breast tomosynthesis compared with full-field digital mammography. British Journal of Radiology, 2019, 92, 20180101.	1.0	7
40	Benign Breast Papilloma without Atypia: Outcomes of Surgical Excision versus US-guided Directional Vacuum-assisted Removal or US Follow-up. Radiology, 2019, 293, 72-80.	3.6	31
41	Predicting Axillary Response to Neoadjuvant Chemotherapy: Breast MRI and US in Patients with Node-Positive Breast Cancer. Radiology, 2019, 293, 49-57.	3.6	60
42	Evaluation of TP53/PIK3CA mutations using texture and morphology analysis on breast MRI. Magnetic Resonance Imaging, 2019, 63, 60-69.	1.0	14
43	Comparison of transcriptome expression alterations by chronic exposure to low-dose bisphenol A in different subtypes of breast cancer cells. Toxicology and Applied Pharmacology, 2019, 385, 114814.	1.3	10
44	Bisphenol A Promotes the Invasive and Metastatic Potential of Ductal Carcinoma In Situ and Protumorigenic Polarization of Macrophages. Toxicological Sciences, 2019, 170, 283-295.	1.4	11
45	Use of Abbreviated Magnetic Resonance Imaging in Breast Cancer Screening. Journal of the Korean Society of Radiology, 2019, 80, 47.	0.1	Ο
46	Detection of axillary lymph node recurrence in patients with personal history of breast cancer treated with sentinel lymph node biopsy (SLNB): results of postoperative combined ultrasound and mammography screening over five consecutive years. Acta Radiologica, 2019, 60, 852-858.	0.5	3
47	Comparison of Ultrasound Elastography and Color Doppler Ultrasonography for Distinguishing Small Tripleâ€Negative Breast Cancer From Fibroadenoma. Journal of Ultrasound in Medicine, 2018, 37, 2135-2146.	0.8	22
48	Contrast-enhanced MRI after neoadjuvant chemotherapy of breast cancer: lesion-to-background parenchymal signal enhancement ratio for discriminating pathological complete response from minimal residual tumour. European Radiology, 2018, 28, 2986-2995.	2.3	31
49	Association between US features of primary tumor and axillary lymph node metastasis in patients with clinical T1–T2N0 breast cancer. Acta Radiologica, 2018, 59, 402-408.	0.5	30
50	Supplemental Screening Breast US in Women with Negative Mammographic Findings: Effect of Routine Axillary Scanning. Radiology, 2018, 286, 830-837.	3.6	16
51	Diagnostic performances of supplemental breast ultrasound screening in women with personal history of breast cancer. Acta Radiologica, 2018, 59, 533-539.	0.5	11
52	Association of preoperative breast MRI features with locoregional recurrence after breast conservation therapy. Acta Radiologica, 2018, 59, 409-417.	0.5	9
53	Construction of a 3D mammary duct based on spatial localization of the extracellular matrix. NPG Asia Materials, 2018, 10, 970-981.	3.8	9
54	IL-6-mediated cross-talk between human preadipocytes and ductal carcinoma in situ in breast cancer progression. Journal of Experimental and Clinical Cancer Research, 2018, 37, 200.	3.5	32

#	Article	IF	CITATIONS
55	Magnetic Resonance Imagingâ€Guided Drug Delivery to Breast Cancer Stem‣ike Cells. Advanced Healthcare Materials, 2018, 7, e1800266.	3.9	17
56	Dynamic Contrast-enhanced Breast MRI for Evaluating Residual Tumor Size after Neoadjuvant Chemotherapy. Radiology, 2018, 289, 327-334.	3.6	52
57	Breast cancer cell-derived exosomes and macrophage polarization are associated with lymph node metastasis. Oncotarget, 2018, 9, 7398-7410.	0.8	104
58	Câ€reactive Protein Binds to Integrin α2 and Fc <sup>î3</sup> receptor I, Leading to Breast Cell Adhesion and Breast Cancer Progression. FASEB Journal, 2018, 32, 533.1.	0.2	0
59	Impact of prior mammograms on combined reading of digital mammography and digital breast tomosynthesis. Acta Radiologica, 2017, 58, 148-155.	0.5	8
60	Prediction of invasive breast cancer using shear-wave elastography in patients with biopsy-confirmed ductal carcinoma in situ. European Radiology, 2017, 27, 7-15.	2.3	31
61	Diagnostic performance of tomosynthesis and breast ultrasonography in women with dense breasts: a prospective comparison study. Breast Cancer Research and Treatment, 2017, 162, 85-94.	1.1	29
62	Background echotexture classification in breast ultrasound: inter-observer agreement study. Acta Radiologica, 2017, 58, 1427-1433.	0.5	17
63	MR imaging features associated with distant metastasis-free survival of patients with invasive breast cancer: a case–control study. Breast Cancer Research and Treatment, 2017, 162, 559-569.	1.1	32
64	Near-infrared photothermal therapy using EGFR-targeted gold nanoparticles increases autophagic cell death in breast cancer. Journal of Photochemistry and Photobiology B: Biology, 2017, 170, 58-64.	1.7	55
65	Breast Cancer Detected at Screening US: Survival Rates and Clinical-Pathologic and Imaging Factors Associated with Recurrence. Radiology, 2017, 284, 354-364.	3.6	28
66	Computer-aided tumor diagnosis using shear wave breast elastography. Ultrasonics, 2017, 78, 125-133.	2.1	21
67	Gene expression profiling of calcifications in breast cancer. Scientific Reports, 2017, 7, 11427.	1.6	21
68	Imaging features of breast cancers on digital breast tomosynthesis according to molecular subtype: association with breast cancer detection. British Journal of Radiology, 2017, 90, 20170470.	1.0	15
69	Interpretation of digital breast tomosynthesis: preliminary study on comparison with picture archiving and communication system (PACS) and dedicated workstation. British Journal of Radiology, 2017, 90, 20170182.	1.0	1
70	Evaluation of Screening US–detected Breast Masses by Combined Use of Elastography and Color Doppler US with B-Mode US in Women with Dense Breasts: A Multicenter Prospective Study. Radiology, 2017, 285, 660-669.	3.6	52
71	Breast Cancer Screening With Mammography Plus Ultrasonography or Magnetic Resonance Imaging in Women 50 Years or Younger at Diagnosis and Treated With Breast Conservation Therapy. JAMA Oncology, 2017, 3, 1495.	3.4	112
72	MR and mammographic imaging features of HER2-positive breast cancers according to hormone receptor status: a retrospective comparative study. Acta Radiologica, 2017, 58, 792-799.	0.5	14

#	Article	IF	CITATIONS
73	Imaging Surveillance for Survivors of Breast Cancer: Correlation between Cancer Characteristics and Method of Detection. Journal of Breast Cancer, 2017, 20, 192.	0.8	1
74	Ultrasound-guided cable-free 13-gauge vacuum-assisted biopsy of non-mass breast lesions. PLoS ONE, 2017, 12, e0179182.	1.1	13
75	Near-infrared photothermal therapy using anti-EGFR-gold nanorod conjugates for triple negative breast cancer. Oncotarget, 2017, 8, 86566-86575.	0.8	29
76	LOXL4 knockdown enhances tumor growth and lung metastasis through collagen-dependent extracellular matrix changes in triple-negative breast cancer. Oncotarget, 2017, 8, 11977-11989.	0.8	46
77	Investigation of discriminant metabolites in tamoxifen-resistant and choline kinase-alpha-downregulated breast cancer cells using 1H-nuclear magnetic resonance spectroscopy. PLoS ONE, 2017, 12, e0179773.	1.1	6
78	microRNA-200c/141 upregulates SerpinB2 to promote breast cancer cell metastasis and reduce patient survival. Oncotarget, 2017, 8, 32769-32782.	0.8	55
79	Can We Skip Intraoperative Evaluation of Sentinel Lymph Nodes? Nomogram Predicting Involvement of Three or More Axillary Lymph Nodes before Breast Cancer Surgery. Cancer Research and Treatment, 2017, 49, 1088-1096.	1.3	24
80	Addition of Digital Breast Tomosynthesis to Full-Field Digital Mammography in the Diagnostic Setting: Additional Value and Cancer Detectability. Journal of Breast Cancer, 2016, 19, 438.	0.8	18
81	Overexpression of the miR-141/200c cluster promotes the migratory and invasive ability of triple-negative breast cancer cells through the activation of the FAK and PI3K/AKT signaling pathways by secreting VEGF-A. BMC Cancer, 2016, 16, 570.	1.1	61
82	Association between Ultrasound Features and the 21-Gene Recurrence Score Assays in Patients with Oestrogen Receptor-Positive, HER2-Negative, Invasive Breast Cancer. PLoS ONE, 2016, 11, e0158461.	1.1	17
83	Different Biological Action of Oleic Acid in ALDHhigh and ALDHlow Subpopulations Separated from Ductal Carcinoma In Situ of Breast Cancer. PLoS ONE, 2016, 11, e0160835.	1.1	3
84	Association between partial-volume corrected SUVmax and Oncotype DX recurrence score in early-stage, ER-positive/HER2-negative invasive breast cancer. European Journal of Nuclear Medicine and Molecular Imaging, 2016, 43, 1574-1584.	3.3	10
85	Replacing single-view mediolateral oblique (MLO) digital mammography (DM) with synthesized mammography (SM) with digital breast tomosynthesis (DBT) images: Comparison of the diagnostic performance and radiation dose with two-view DM with or without MLO-DBT. European Journal of Radiology, 2016, 85, 2042-2048.	1.2	12
86	Pretreatment MR Imaging Features of Triple-Negative Breast Cancer: Association with Response to Neoadjuvant Chemotherapy and Recurrence-Free Survival. Radiology, 2016, 281, 392-400.	3.6	100
87	Ultrasound-guided photoacoustic imaging for the selective detection of EGFR-expressing breast cancer and lymph node metastases. Biomedical Optics Express, 2016, 7, 1920.	1.5	24
88	Residual Mammographic Microcalcifications and Enhancing Lesions on MRI After Neoadjuvant Systemic Chemotherapy for Locally Advanced Breast Cancer: Correlation with Histopathologic Residual Tumor Size. Annals of Surgical Oncology, 2016, 23, 1135-1142.	0.7	35
89	Early prediction of response to neoadjuvant chemotherapy in breast cancer patients: comparison of single-voxel 1H-magnetic resonance spectroscopy and 18F-fluorodeoxyglucose positron emission tomography. European Radiology, 2016, 26, 2279-2290.	2.3	14
90	Comparison of the diagnostic performance of digital breast tomosynthesis and magnetic resonance imaging added to digital mammography in women with known breast cancers. European Radiology, 2016, 26, 1556-1564.	2.3	32

#	Article	IF	CITATIONS
91	A novel role for flotillinâ€1 in <scp>H</scp> â€ <scp>R</scp> asâ€regulated breast cancer aggressiveness. International Journal of Cancer, 2016, 138, 1232-1245.	2.3	24
92	Early Stage Triple-Negative Breast Cancer: Imaging and Clinical-Pathologic Factors Associated with Recurrence. Radiology, 2016, 278, 356-364.	3.6	42
93	Breast Magnetic Resonance Imaging-Guided Biopsy. Journal of the Korean Society of Radiology, 2016, 74, 351.	0.1	2
94	Quantitative analysis of breast echotexture patterns in automated breast ultrasound images. Medical Physics, 2015, 42, 4566-4578.	1.6	10
95	Targeted Therapy for Breast Cancer Stem Cells by Liposomal Delivery of siRNA against Fibronectin EDB. Advanced Healthcare Materials, 2015, 4, 1675-1680.	3.9	27
96	Characterization of Breast Lesions: Comparison of Digital Breast Tomosynthesis and Ultrasonography. Korean Journal of Radiology, 2015, 16, 229.	1.5	34
97	Downregulation of Choline Kinase-Alpha Enhances Autophagy in Tamoxifen-Resistant Breast Cancer Cells. PLoS ONE, 2015, 10, e0141110.	1.1	14
98	Correlation between 18F-FDG uptake on PET/CT and prognostic factors in triple-negative breast cancer. European Radiology, 2015, 25, 3314-3321.	2.3	34
99	Heterogeneity of triple-negative breast cancer: mammographic, US, and MR imaging features according to androgen receptor expression. European Radiology, 2015, 25, 419-427.	2.3	23
100	An Artificial Immune System-Based Support Vector Machine Approach for Classifying Ultrasound Breast Tumor Images. Journal of Digital Imaging, 2015, 28, 576-585.	1.6	25
101	Undiagnosed Breast Cancer: Features at Supplemental Screening US. Radiology, 2015, 277, 372-380.	3.6	24
102	Automated breast ultrasound system (ABUS): reproducibility of mass localization, size measurement, and characterization on serial examinations. Acta Radiologica, 2015, 56, 1163-1170.	0.5	37
103	A microengineered pathophysiological model of early-stage breast cancer. Lab on A Chip, 2015, 15, 3350-3357.	3.1	174
104	Quantitative MRI morphology of invasive breast cancer: correlation with immunohistochemical biomarkers and subtypes. Acta Radiologica, 2015, 56, 269-275.	0.5	46
105	Radiologist-performed hand-held ultrasound screening at average risk of breast cancer: results from a single health screening center. Acta Radiologica, 2015, 56, 652-658.	0.5	41
106	Intensity-Invariant Texture Analysis for Classification of BI-RADS Category 3 Breast Masses. Ultrasound in Medicine and Biology, 2015, 41, 2039-2048.	0.7	27
107	Breast Cancer Recurrence in Patients with Newly Diagnosed Breast Cancer without and with Preoperative MR Imaging: A Matched Cohort Study. Radiology, 2015, 276, 695-705.	3.6	36
108	Shear-Wave Elastography for the Detection of Residual Breast Cancer After Neoadjuvant Chemotherapy. Annals of Surgical Oncology, 2015, 22, 376-384.	0.7	25

#	Article	IF	CITATIONS
109	Ultrasound screening of contralateral breast after surgery for breast cancer. European Journal of Radiology, 2015, 84, 54-60.	1.2	14
110	Noninvasive MRI and multilineage differentiation capability of ferritinâ€ŧransduced human mesenchymal stem cells. NMR in Biomedicine, 2015, 28, 168-179.	1.6	15
111	Location of Triple-Negative Breast Cancers: Comparison with Estrogen Receptor-Positive Breast Cancers on MR Imaging. PLoS ONE, 2015, 10, e0116344.	1.1	9
112	In vivo Tracking of Dendritic Cell using MRI Reporter Gene, Ferritin. PLoS ONE, 2015, 10, e0125291.	1.1	32
113	Correlation between tumor-free axillary lymph node morphology and clinicopathologic features in invasive breast cancer Journal of Clinical Oncology, 2015, 33, e12059-e12059.	0.8	0
114	Intratumoral Heterogeneity of Breast Cancer Xenograft Models: Texture Analysis of Diffusion-Weighted MR Imaging. Korean Journal of Radiology, 2014, 15, 591.	1.5	27
115	Real-Time Imaging of the Epithelial-Mesenchymal Transition Using microRNA-200a Sequence-Based Molecular Beacon-Conjugated Magnetic Nanoparticles. PLoS ONE, 2014, 9, e102164.	1.1	11
116	Low Rates of Additional Cancer Detection by Magnetic Resonance Imaging in Newly Diagnosed Breast Cancer Patients Who Undergo Preoperative Mammography and Ultrasonography. Journal of Breast Cancer, 2014, 17, 167.	0.8	15
117	Practice guideline for the performance of breast ultrasound elastography. Ultrasonography, 2014, 33, 3-10.	1.0	79
118	MRI of Breast Tumor Initiating Cells Using the Extra Domain-B of Fibronectin Targeting Nanoparticles. Theranostics, 2014, 4, 845-857.	4.6	28
119	A New Full-Field Digital Mammography System with and without the Use of an Advanced Post-Processing Algorithm: Comparison of Image Quality and Diagnostic Performance. Korean Journal of Radiology, 2014, 15, 305.	1.5	5
120	Added Value of Shear-Wave Elastography for Evaluation of Breast Masses Detected with Screening US Imaging. Radiology, 2014, 273, 61-69.	3.6	105
121	Breast Cancer: Early Prediction of Response to Neoadjuvant Chemotherapy Using Parametric Response Maps for MR Imaging. Radiology, 2014, 272, 385-396.	3.6	81
122	Breast MR Imaging Screening in Women with a History of Breast Conservation Therapy. Radiology, 2014, 272, 366-373.	3.6	81
123	Tumor detection in automated breast ultrasound images using quantitative tissue clustering. Medical Physics, 2014, 41, 042901.	1.6	50
124	Shear-Wave Elastographic Features of Breast Cancers. Investigative Radiology, 2014, 49, 147-155.	3.5	39
125	18F-FDG uptake in breast cancer correlates with immunohistochemically defined subtypes. European Radiology, 2014, 24, 610-618.	2.3	81
126	Correlation of breast cancer subtypes, based on estrogen receptor, progesterone receptor, and HER2, with functional imaging parameters from 68Ga-RGD PET/CT and 18F-FDG PET/CT. European Journal of Nuclear Medicine and Molecular Imaging, 2014, 41, 1534-1543.	3.3	65

#	Article	IF	CITATIONS
127	Tumour volume doubling time of molecular breast cancer subtypes assessed by serial breast ultrasound. European Radiology, 2014, 24, 2227-2235.	2.3	66
128	Quantitative Analysis for Breast Density Estimation in Low Dose Chest CT Scans. Journal of Medical Systems, 2014, 38, 21.	2.2	15
129	Two-View versus Single-View Shear-Wave Elastography: Comparison of Observer Performance in Differentiating Benign from Malignant Breast Masses. Radiology, 2014, 270, 344-353.	3.6	53
130	Breast Cancer Detected with Screening US: Reasons for Nondetection at Mammography. Radiology, 2014, 270, 369-377.	3.6	136
131	Usefulness of ultrasound elastography in reducing the number of Breast Imaging Reporting and Data System category 3 lesions on ultrasonography. Ultrasonography, 2014, 33, 98-104.	1.0	10
132	Shear-wave elastography in detection of residual breast cancer after neoadjuvant chemotherapy Journal of Clinical Oncology, 2014, 32, 102-102.	0.8	0
133	Triple-negative invasive breast cancer (TNBC): Mammographic, US, and MR imaging features according to androgen receptor (AR) expression Journal of Clinical Oncology, 2014, 32, 159-159.	0.8	0
134	Comparison of Shear-Wave and Strain Ultrasound Elastography in the Differentiation of Benign and Malignant Breast Lesions. American Journal of Roentgenology, 2013, 201, W347-W356.	1.0	154
135	Predictive value of FDG PET/CT for pathologic axillary node involvement after neoadjuvant chemotherapy. Breast Cancer, 2013, 20, 167-173.	1.3	17
136	Association of Tumour Stiffness on Sonoelastography with Axillary Nodal Status in T1 Breast Carcinoma Patients. European Radiology, 2013, 23, 2979-2987.	2.3	21
137	Stiffness of tumours measured by shear-wave elastography correlated with subtypes of breast cancer. European Radiology, 2013, 23, 2450-2458.	2.3	143
138	Mammographic features of calcifications in DCIS: correlation with oestrogen receptor and human epidermal growth factor receptor 2 status. European Radiology, 2013, 23, 2072-2078.	2.3	28
139	Differentiation of benign from malignant solid breast masses: comparison of two-dimensional and three-dimensional shear-wave elastography. European Radiology, 2013, 23, 1015-1026.	2.3	106
140	Automatic detection of microcalcifications in breast ultrasound. Medical Physics, 2013, 40, 102901.	1.6	8
141	Ultrasonographic assessment of breast density. Breast Cancer Research and Treatment, 2013, 138, 851-859.	1.1	21
142	Quantitative Ultrasound Analysis for Classification of BI-RADS Category 3 Breast Masses. Journal of Digital Imaging, 2013, 26, 1091-1098.	1.6	47
143	Robust Texture Analysis Using Multi-Resolution Gray-Scale Invariant Features for Breast Sonographic Tumor Diagnosis. IEEE Transactions on Medical Imaging, 2013, 32, 2262-2273.	5.4	82
144	Computer-Aided Tumor Detection Based on Multi-Scale Blob Detection Algorithm in Automated Breast Ultrasound Images. IEEE Transactions on Medical Imaging, 2013, 32, 1191-1200.	5.4	93

#	Article	IF	CITATIONS
145	In Vivo Magnetic Resonance Imaging of Transgenic Mice Expressing Human Ferritin. Molecular Imaging and Biology, 2013, 15, 48-57.	1.3	14
146	Classification of Breast Tumors Using Elastographic and B-mode Features: Comparison of Automatic Selection of Representative Slice and Physician-Selected Slice of Images. Ultrasound in Medicine and Biology, 2013, 39, 1147-1157.	0.7	13
147	Computer-aided diagnosis of breast masses using quantified BI-RADS findings. Computer Methods and Programs in Biomedicine, 2013, 111, 84-92.	2.6	44
148	Changes in Metabolic Markers in Insulin-Producing Î <sup>2</sup> -Cells during Hypoxia-Induced Cell Death As Studied by NMR Metabolomics. Journal of Proteome Research, 2013, 12, 3738-3745.	1.8	8
149	Unilateral Breast Cancer: Screening of Contralateral Breast by Using Preoperative MR Imaging Reduces Incidence of Metachronous Cancer. Radiology, 2013, 267, 57-66.	3.6	56
150	Rapid Breast Density Analysis of Partial Volumes of Automated Breast Ultrasound Images. Ultrasonic Imaging, 2013, 35, 333-343.	1.4	10
151	Sonoelastography in Distinguishing Benign from Malignant Complex Breast Mass and Making the Decision to Biopsy. Korean Journal of Radiology, 2013, 14, 559.	1.5	24
152	Noninvasive Identification of Viable Cell Populations in Docetaxel-Treated Breast Tumors Using Ferritin-Based Magnetic Resonance Imaging. PLoS ONE, 2013, 8, e52931.	1.1	21
153	Discordant ER, PR, and HER2 status between primary and metastatic breast cancer as prognostic factor Journal of Clinical Oncology, 2013, 31, 1039-1039.	0.8	28
154	Two-View versus Single-View Shear-Wave Elastography: Comparison of Observer Performance in Differentiating Benign from Malignant Breast Masses. Radiology, 2013, , 130561.	3.6	1
155	Distinguishing Benign from Malignant Masses at Breast US: Combined US Elastography and Color Doppler US—Influence on Radiologist Accuracy. Radiology, 2012, 262, 80-90.	3.6	134
156	Computerâ€∎ided classification of breast masses using speckle features of automated breast ultrasound images. Medical Physics, 2012, 39, 6465-6473.	1.6	38
157	Comparison of Two Ultrasmall Superparamagnetic Iron Oxides on Cytotoxicity and MR Imaging of Tumors. Theranostics, 2012, 2, 76-85.	4.6	55
158	Computer-Aided Diagnosis Based on Speckle Patterns in Ultrasound Images. Ultrasound in Medicine and Biology, 2012, 38, 1251-1261.	0.7	21
159	Combining support vector machine with genetic algorithm to classify ultrasound breast tumor images. Computerized Medical Imaging and Graphics, 2012, 36, 627-633.	3.5	77
160	Theranostic Probe Based on Lanthanideâ€Doped Nanoparticles for Simultaneous In Vivo Dualâ€Modal Imaging and Photodynamic Therapy. Advanced Materials, 2012, 24, 5755-5761.	11.1	367
161	Macrophages Homing to Metastatic Lymph Nodes Can Be Monitored with Ultrasensitive Ferromagnetic Iron-Oxide Nanocubes and a 1.5T Clinical MR Scanner. PLoS ONE, 2012, 7, e29575.	1.1	14
162	Correlation of perfusion parameters on dynamic contrastâ€enhanced MRI with prognostic factors and subtypes of breast cancers. Journal of Magnetic Resonance Imaging, 2012, 36, 145-151.	1.9	123

#	Article	IF	CITATIONS
163	Synthesis of Uniformly Sized Manganese Oxide Nanocrystals with Various Sizes and Shapes and Characterization of Their <i>T</i> <sub>1</sub> Magnetic Resonance Relaxivity. European Journal of Inorganic Chemistry, 2012, 2012, 2148-2155.	1.0	71
164	Water-Dispersible Ferrimagnetic Iron Oxide Nanocubes with Extremely High <i>r</i> <sub>2</sub> Relaxivity for Highly Sensitive in Vivo MRI of Tumors. Nano Letters, 2012, 12, 3127-3131.	4.5	269
165	Comparison of diffusion-weighted MR imaging and FDG PET/CT to predict pathological complete response to neoadjuvant chemotherapy in patients with breast cancer. European Radiology, 2012, 22, 18-25.	2.3	91
166	Sonoelastography for 1786 non-palpable breast masses: diagnostic value in the decision to biopsy. European Radiology, 2012, 22, 1033-1040.	2.3	81
167	Detection of prostaglandin E2â€induced dendritic cell migration into the lymph nodes of mice using a 1.5 T clinical MR scanner. NMR in Biomedicine, 2012, 25, 570-579.	1.6	6
168	Cardiac Transcription Factor Nkx2.5 Is Downregulated under Excessive O-GlcNAcylation Condition. PLoS ONE, 2012, 7, e38053.	1.1	13
169	Breast Cancer Screening with MRI. Journal of the Korean Society of Magnetic Resonance in Medicine, 2012, 16, 1.	0.1	0
170	Breast density change as a predictive surrogate for response to adjuvant endocrine therapy in estrogen receptor-positive breast cancer Journal of Clinical Oncology, 2012, 30, e21160-e21160.	0.8	0
171	Breast-conserving surgery after neoadjuvant chemotherapy for stage III breast cancer patients Journal of Clinical Oncology, 2012, 30, e11532-e11532.	0.8	0
172	Comparative study of density analysis using automated whole breast ultrasound and MRI. Medical Physics, 2011, 38, 382-389.	1.6	39
173	Large-Scale Synthesis of Bioinert Tantalum Oxide Nanoparticles for X-ray Computed Tomography Imaging and Bimodal Image-Guided Sentinel Lymph Node Mapping. Journal of the American Chemical Society, 2011, 133, 5508-5515.	6.6	316
174	Large-Scale Synthesis of Uniform and Extremely Small-Sized Iron Oxide Nanoparticles for High-Resolution <i>T</i> <sub>1</sub> Magnetic Resonance Imaging Contrast Agents. Journal of the American Chemical Society, 2011, 133, 12624-12631.	6.6	835
175	Radiologists' performance in the detection of benign and malignant masses with 3D automated breast ultrasound (ABUS). European Journal of Radiology, 2011, 78, 99-103.	1.2	52
176	Characteristics of breast cancers detected by ultrasound screening in women with negative mammograms. Cancer Science, 2011, 102, 1862-1867.	1.7	39
177	Sonoelastographic lesion stiffness: preoperative predictor of the presence of an invasive focus in nonpalpable DCIS diagnosed at US-guided needle biopsy. European Radiology, 2011, 21, 1618-1627.	2.3	22
178	Papillary Lesions Initially Diagnosed at Ultrasound-guided Vacuum-assisted Breast Biopsy: Rate of Malignancy Based on Subsequent Surgical Excision. Annals of Surgical Oncology, 2011, 18, 2506-2514.	0.7	75
179	Clinical application of shear wave elastography (SWE) in the diagnosis of benign and malignant breast diseases. Breast Cancer Research and Treatment, 2011, 129, 89-97.	1.1	300
180	Computer-Aided Diagnosis for the Classification of Breast Masses in Automated Whole Breast Ultrasound Images. Ultrasound in Medicine and Biology, 2011, 37, 539-548.	0.7	84

#	Article	IF	CITATIONS
181	Breast Tumor Classification Using Fuzzy Clustering for Breast Elastography. Ultrasound in Medicine and Biology, 2011, 37, 700-708.	0.7	48
182	Breast Mass Evaluation: Factors Influencing the Quality of US Elastography. Radiology, 2011, 259, 59-64.	3.6	165
183	Magnetosome-like ferrimagnetic iron oxide nanocubes for highly sensitive MRI of single cells and transplanted pancreatic islets. Proceedings of the National Academy of Sciences of the United States of America, 2011, 108, 2662-2667.	3.3	183
184	Aliasing artifact depicted on ultrasound (US)-elastography for breast cystic lesions mimicking solid masses. Acta Radiologica, 2011, 52, 3-7.	0.5	27
185	An HR-MAS MR Metabolomics Study on Breast Tissues Obtained with Core Needle Biopsy. PLoS ONE, 2011, 6, e25563.	1.1	66
186	Sonoelastographic Strain Index for Differentiation of Benign and Malignant Nonpalpable Breast Masses. Journal of Ultrasound in Medicine, 2010, 29, 1-7.	0.8	136
187	Risk of carcinoma after subsequent excision of benign papilloma initially diagnosed with an ultrasound (US)-guided 14-gauge core needle biopsy: a prospective observational study. European Radiology, 2010, 20, 1093-1100.	2.3	63
188	The effects of clinically used MRI contrast agents on the biological properties of human mesenchymal stem cells. NMR in Biomedicine, 2010, 23, 514-522.	1.6	62
189	Diffusion-weighted MR Imaging: Pretreatment Prediction of Response to Neoadjuvant Chemotherapy in Patients with Breast Cancer. Radiology, 2010, 257, 56-63.	3.6	249
190	<i>In vivo</i> Imaging of Tumor Transduced with Bimodal Lentiviral Vector Encoding Human Ferritin and Green Fluorescent Protein on a 1.5T Clinical Magnetic Resonance Scanner. Cancer Research, 2010, 70, 7315-7324.	0.4	60
191	Integrin-targeting thermally cross-linked superparamagnetic iron oxide nanoparticles for combined cancer imaging and drug delivery. Nanotechnology, 2010, 21, 415102.	1.3	52
192	Differentiation of benign from malignant nonpalpable breast masses: A comparison of computer-assisted quantification and visual assessment of lesion stiffness with the use of sonographic elastography. Acta Radiologica, 2010, 51, 9-14.	0.5	31
193	Uniform Mesoporous Dye-Doped Silica Nanoparticles Decorated with Multiple Magnetite Nanocrystals for Simultaneous Enhanced Magnetic Resonance Imaging, Fluorescence Imaging, and Drug Delivery. Journal of the American Chemical Society, 2010, 132, 552-557.	6.6	687
194	Detection of Microcalcifications in Digital Mammograms Using Foveal Method. Journal of Korean Society of Medical Informatics, 2009, 15, 165.	0.3	7
195	Preoperative Sonographic Classification of Axillary Lymph Nodes in Patients With Breast Cancer: Node-to-Node Correlation With Surgical Histology and Sentinel Node Biopsy Results. American Journal of Roentgenology, 2009, 193, 1731-1737.	1.0	115
196	Nonblinking and Nonbleaching Upconverting Nanoparticles as an Optical Imaging Nanoprobe and T1 Magnetic Resonance Imaging Contrast Agent. Advanced Materials, 2009, 21, 4467-4471.	11.1	548
197	Analysis of Elastographic and B-mode Features at Sonoelastography for Breast Tumor Classification. Ultrasound in Medicine and Biology, 2009, 35, 1794-1802.	0.7	56
198	Real-time US elastography in the differentiation of suspicious microcalcifications on mammography. European Radiology, 2009, 19, 1621-1628.	2.3	45

#	Article	IF	CITATIONS
199	Characterizing time-intensity curves for spectral morphometric analysis of intratumoral enhancement patterns in breast DCE-MRI: Comparison between differentiation performance of temporal model parameters based on DFT and SVD. , 2009, , .		4
200	Various-Shaped Uniform Mn <sub>3</sub> O <sub>4</sub> Nanocrystals Synthesized at Low Temperature in Air Atmosphere. Chemistry of Materials, 2009, 21, 2272-2279.	3.2	135
201	Scoring system for predicting malignancy in patients diagnosed with atypical ductal hyperplasia at ultrasound-guided core needle biopsy. Breast Cancer Research and Treatment, 2008, 112, 189-195.	1.1	71
202	Tamper Detection and Recovery for Medical Images Using Near-lossless Information Hiding Technique. Journal of Digital Imaging, 2008, 21, 59-76.	1.6	89
203	Analysis of Tumor Vascularity Using Three-Dimensional Power Doppler Ultrasound Images. IEEE Transactions on Medical Imaging, 2008, 27, 320-330.	5.4	70
204	Simple and Generalized Synthesis of Oxideâ^'Metal Heterostructured Nanoparticles and their Applications in Multimodal Biomedical Probes. Journal of the American Chemical Society, 2008, 130, 15573-15580.	6.6	162
205	Texture analysis of lesion perfusion volumes in dynamic contrast-enhanced breast MRI. , 2008, , .		4
206	Synthesis of Uniform Hollow Oxide Nanoparticles through Nanoscale Acid Etching. Nano Letters, 2008, 8, 4252-4258.	4.5	210
207	Ultrasound Breast Tumor Image Computer-Aided Diagnosis With Texture and Morphological Features. Academic Radiology, 2008, 15, 873-880.	1.3	52
208	Nonpalpable Breast Masses: Evaluation by US Elastography. Korean Journal of Radiology, 2008, 9, 111.	1.5	118
209	Correlation between High Resolution Dynamic MR Features and Prognostic Factors in Breast Cancer. Korean Journal of Radiology, 2008, 9, 10.	1.5	113
210	Screening Mammography–detected Cancers: Sensitivity of a Computer-aided Detection System Applied to Full-Field Digital Mammograms. Radiology, 2007, 244, 104-111.	3.6	70
211	Breast Ultrasound Computer-Aided Diagnosis Using BI-RADS Features. Academic Radiology, 2007, 14, 928-939.	1.3	111
212	The Role of PET/CT for Evaluating Breast Cancer. Korean Journal of Radiology, 2007, 8, 429.	1.5	59
213	Labeling Efficacy of Superparamagnetic Iron Oxide Nanoparticles to Human Neural Stem Cells: Comparison of Ferumoxides, Monocrystalline Iron Oxide, Cross-linked Iron Oxide (CLIO)-NH2 and tat-CLIO. Korean Journal of Radiology, 2007, 8, 365.	1.5	65
214	MRI of the Breast for the Detection and Assessment of the Size of Ductal Carcinoma in Situ. Korean Journal of Radiology, 2007, 8, 32.	1.5	62
215	Analysis of Previous Screening Examinations for Patients with Breast Cancer. Journal of the Korean Radiological Society, 2007, 56, 191.	0.0	2
216	Breast Imaging Reporting and Data System (BI-RADS) US lexicon and Final Assessment Category for Solid Breast Masses: the Rates of Inter- and Intraobserver Agreement. Journal of the Korean Radiological Society, 2007, 56, 593.	0.0	1

#	Article	IF	CITATIONS
217	Differentiating Benign from Malignant Solid Breast Masses: Comparison of Two-dimensional and Three-dimensional US. Radiology, 2006, 240, 26-32.	3.6	56
218	Breast Density Analysis in 3-D Whole Breast Ultrasound Images. Annual International Conference of the IEEE Engineering in Medicine and Biology Society, 2006, , .	0.5	0
219	Three Comparative Approaches for Breast Density Estimation in Digital and Screen Film Mammograms. Annual International Conference of the IEEE Engineering in Medicine and Biology Society, 2006, , .	0.5	0
220	Classification of breast ultrasound images using fractal feature. Clinical Imaging, 2005, 29, 235-245.	0.8	130
221	Automatic ultrasound segmentation and morphology based diagnosis of solid breast tumors. Breast Cancer Research and Treatment, 2005, 89, 179-185.	1.1	188
222	Sonographically Guided Core Biopsy of the Breast: Comparison of 14-Gauge Automated Gun and 11-Gauge Directional Vacuum-Assisted Biopsy Methods. Korean Journal of Radiology, 2005, 6, 102.	1.5	65
223	Solid Breast Masses: Classification with Computer-aided Analysis of Continuous US Images Obtained with Probe Compression. Radiology, 2005, 236, 458-464.	3.6	57
224	Differentiation of Benign from Malignant Solid Breast Masses: Conventional US versus Spatial Compound Imaging. Radiology, 2005, 237, 841-846.	3.6	57
225	Reproducibility of Computer-Aided Detection System in Digital Mammograms. Journal of the Korean Radiological Society, 2005, 52, 137.	0.0	3
226	Comparative evaluation of three superparamagnetic iron oxide nanoparticles, feridex, MION-47, and tat-CLIO, to label human neural stem cells. Journal of Cerebral Blood Flow and Metabolism, 2005, 25, S514-S514.	2.4	0
227	Characterization of Spiculation on Ultrasound Lesions. IEEE Transactions on Medical Imaging, 2004, 23, 111-121.	5.4	43
228	Computer-Aided Diagnosis of Solid Breast Nodules: Use of an Artificial Neural Network Based on Multiple Sonographic Features. IEEE Transactions on Medical Imaging, 2004, 23, 1292-1300.	5.4	223
229	Improvement in breast tumor discrimination by support vector machines and speckle-emphasis texture analysis. Ultrasound in Medicine and Biology, 2003, 29, 679-686.	0.7	123
230	3-D breast ultrasound segmentation using active contour model. Ultrasound in Medicine and Biology, 2003, 29, 1017-1026.	0.7	85
231	Segmentation of breast tumor in three-dimensional ultrasound images using three-dimensional discrete active contour model. Ultrasound in Medicine and Biology, 2003, 29, 1571-1581.	0.7	56
232	Support Vector Machines for Diagnosis of Breast Tumors on US Images. Academic Radiology, 2003, 10, 189-197.	1.3	104
233	Enhanced Tumor Detection Using a Folate Receptor-Targeted Near-Infrared Fluorochrome Conjugate. Bioconjugate Chemistry, 2003, 14, 539-545.	1.8	121
234	Pregnancy- and Lactation-Associated Breast Cancer. Journal of Ultrasound in Medicine, 2003, 22, 491-497.	0.8	130

#	Article	IF	CITATIONS
235	Multifocal, Multicentric, and Contralateral Breast Cancers: Bilateral Whole-Breast US in the Preoperative Evaluation of Patients. Radiology, 2002, 224, 569-576.	3.6	134
236	US of Ductal Carcinoma In Situ. Radiographics, 2002, 22, 269-281.	1.4	107
237	Computer-Aided Diagnosis of Breast Tumors with Different US Systems. Academic Radiology, 2002, 9, 793-799.	1.3	56
238	A Receptor-Targeted Near-Infrared Fluorescence Probe for In Vivo Tumor Imaging. ChemBioChem, 2002, 3, 784.	1.3	110
239	Retrieval technique for the diagnosis of solid breast tumors on sonogram. Ultrasound in Medicine and Biology, 2002, 28, 903-909.	0.7	49
240	Fluorodeoxyglucose positron emission tomography for detection of recurrent or metastatic breast cancer. World Journal of Surgery, 2001, 25, 829-834.	0.8	59
241	Metaplastic carcinoma of the breast: Mammographic and sonographic findings. , 2000, 28, 179-186.		66
242	US of Mammographically Detected Clustered Microcalcifications. Radiology, 2000, 217, 849-854.	3.6	150
243	Nonpalpable Breast Lesions: Evaluation with Power Doppler US and a Microbubble Contrast Agent—Initial Experience. Radiology, 2000, 217, 240-246.	3.6	92
244	Complications of Klebsiella Pneumonia. Journal of Computer Assisted Tomography, 1995, 19, 176-181.	0.5	45
245	Mediastinal Castleman Disease. Journal of Computer Assisted Tomography, 1994, 18, 43-46.	0.5	41
246	Breast ultrasound image classification using fractal analysis. , 0, , .		7
247	The Usefulness of Ultrasound Surveillance for Axillary Recurrence in Women With Personal History of Breast Cancer. Journal of Breast Cancer, 0, 24, .	0.8	0